Neutrinoless double beta decay and nuclear matrix elements

P. K. Raina[a]
Department of Physics, Indian Institute of Technology Ropar
Rupnagar 140001, INDIA

Neutrinoless double beta decay is the only experiment at present promising to settle the Majorana/ Dirac nature of neutrino and is being pursued by a few groups globally. Apart from establishing Majorana character of neutrinos this experiment is also most sensitive to look for the neutrino mass and establish lepton number violation. However, in the process of extraction of neutrino mass from half life measurement one has to use the nuclear transition matrix elements for the nuclei involved. Studies in different models for nuclear matrix elements calculations in general are discussed and the connected uncertainties too are reported.

1 Introduction

Confirmation of neutrino oscillations in different experiments [1] has established the massive character of neutrino and served as a strong evidence to look beyond the well-accepted standard model of particles. Most of the unified theories thus evolved are based on Majorana character of neutrinos. It was realized almost eighty years back that neutrinoless double beta decay (DBD) is one of the best possible experiments to explore the nature of neutrino [2]. Intermittent attempts have been made since then but only after first successful direct experimental observation for ^{82}Se in 1987 the measurements of half lives for two neutrino DBD ware taken up seriously in the decades of 80s and 90s. As a result, now it is known for almost a dozen nuclei in the range of 10^{19} to 10^{22} yrs. In 2004, a controversial HdM measurement [3] on neutrinoless DBD of ^{76}Ge was reported in the order of 10^{25} yrs. Since then quite a few attempts are being made to achieve the expected half lives predicted in this order. Recently [4] some experiments have achieved this range of measurements and have plans to go an order or two higher that would correspond to the mass of neutrino in 10s or 100s of meV ranges. At present neutrinoless DBD is the only experiment promising to disclose the Majorana/ Dirac nature of neutrino and is being pursued rigorously by different groups (reviewed in Refs. [5,6]).

Different theoretical models and approaches used for extraction of nuclear matrix elements (NMEs) play crucial role in arriving at the value of neutrino mass from neutrinoless DBD half life. We have presented brief summary of these models and some of our calculations in deformed HF and projected HFB models in subsequent sections. Physically important considerations to address the variations in NMEs that have been discussed in literature recently are also presented [7]. Calculations of NMEs in general are presented and the connected uncertainties in particular for QRPA and PHFB are reported towards the end. We conclude with the important future considerations to be addressed urgently in near future by theoreticians.

[a] The present work is done in collaboration with P. K. Rath (Univ. of Lucknow, India), S. K. Ghorui (IIT Ropar, India), R. Chandra (BBA Univ., Lucknow, India), K. Chaturvedi (Bundelkhand Univ., Jhansi, India) and J. G. Hirsch (Universidad Nacional Autonona de Mexico)

2 Nuclear Models

A variety of nuclear models is currently employed for the study of double beta decay. Large scale shell model calculations are the most desirable approach [8], but highly limited in the description of medium and heavy mass nuclei. The most popular and successful model is the Quasiparticle Random Phase Approximation (QRPA) and its extensions [9,10]. The inclusion of nuclear deformation has also been carried out in the deformed QRPA [11], the Projected Hartree-Fock-Bogoliubov (PHFB) [12], the Interacting Boson Model (IBM) [13], and the Energy Density Functional (EDF) [14] approaches. The relative applicability and shortcomings of the various models are discussed in more details in Refs. [6,7,9]. Below, we briefly discuss about different models for the completeness.
The Nuclear Shell Model (NSM): The NSM tries to solve the nuclear many-body problem as accurate as possible and correlations are treated exactly. However, only a limited number of orbits close to the Fermi levels are considered. The effective interactions are usually constructed starting from monopole corrected G-matrices or through a renormalization-group treatment.
The Quasiparticle Random Phase Approximation (QRPA): The QRPA and its extensions have emerged as successful model as it include large number of basis space. On the otherhand, all correlations are not included. The particle numbers are not exactly conserved as proton-proton and neutron-neutron pairings are treated in the BCS approximation. The many-body correlations are treated at the RPA level within the quasiboson approximation.
The Projected Hartree-Fock-Bogoliubov Method (PHFB): In the PHFB wave functions of good particle number and angular momentum are obtained by projection on the axially symmetric intrinsic HFB states. In applications to the calculation of the $0\nu\beta\beta$-decay NMEs, the effective Hamiltonian contains terms which are separable in the pairing, quadrupole, and hexadecupole channels.
The Interacting Boson Model (IBM-2): In IBM model the nucleon pair are represented by bosons with angular momentum either L=0 (s boson) or L=2 (d boson). The interacting potential of bosons acts only in pair which is analogous to the Shell Model. The bosons interact through one- and two-body forces giving rise to bosonic wave functions.
The Energy Density Functional (EDF) Method: The EDF method is based on HFB calculations with density dependent Gogny functional. It is an improved method with respect to the PHFB model. The particle number and angular momentum projection for parent and daughter nuclei is performed. Configuration mixing within the generating coordinate method (GCM) is included to take into account beyond mean-field effects. A large single particle basis is considered in the calculations.

3 Results and Discussions

3.1 2ν ββ decay

The nuclear $\beta\beta$ decay is a second order process in weak interaction. The inverse half-life of the 2ν $\beta\beta$ decay for the $0^+ \rightarrow 0^+$ transition can be written as [15]

$$[T^{2\nu}_{1/2}(0^+ \rightarrow 0^+)]^{-1} = G_{2\nu} \left| M_{2\nu} \right|^2 \quad , \tag{1}$$

where $G_{2\nu}$ is the integrated kinematical factor and can be calculated with good accuracy [15,16]. Using the experimental half-life $T^{2\nu}_{1/2}$ and accurately known integrated kinematical factor $G_{2\nu}$, the values of $M_{2\nu}$ can be extracted directly from Eq. (1). It is observed that in all cases of 2ν $\beta^-\beta^-$ decay, the double Gamow-Teller (DGT) transition matrix elements $M_{2\nu}$ are sufficiently quenched. The main motive of all theoretical calculations is to understand the physical mechanism responsible for the observed suppression of $M_{2\nu}$. Hence, the validity of different nuclear models can be tested through the calculation of $M_{2\nu}$.

In Fig. 1, we present a compilation of the magnitude of double beta decay matrix elements calculated within Deformed Hartree-Fock (DHF) model for 0^+(gs) $\rightarrow$ 0^+(gs) transition of the

nuclei studied presently. The purpose of this pictorial representation is for better viewing of the matrix elements calculated within different formalisms and their comparison with the values extracted from average/ recommended experimental half-lives given by Barabash [17] for $g_A = 1.254$ and $g_A = 1.0$. However, these values are updated very recently [18] and we will incorporate them in our future study. From Fig. 1, we see that there is considerably large variation in the $M^{2\nu}$ values calculated within different models. Therefore, it is very difficult to draw a systematic trend for NTMEs.

From the above discussion it is clear that the validity of nuclear models presently employed to calculate two neutrino double beta decay transition matrix elements ($M^{2\nu}$) cannot be uniquely established. It is also to be noted that the value of axial- vector coupling constant g_A plays vital part in the uncertainty of calculated half-lives as the rate of double beta decay varies on $(g_A)^4$. The renormalized or quenched value of $g_A = 1.0$ is taken in order to include the nuclear core (medium) effects such as the spin-isospin correlations. To fine tune the quenching of g_A value, the charge exchange reaction experiments involving the double beta decay nuclei or the nuclei in the vicinity of $\beta\beta$ emitters can play important role.

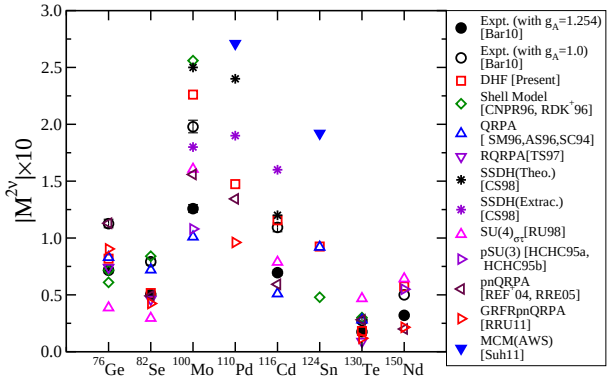

Figure 1 – Comparison of calculated NTMEs with available experimental results for $2\nu\ \beta^-\beta^-$ decay of ^{76}Ge, ^{82}Se, ^{100}Mo, ^{110}Pd, ^{116}Cd, ^{124}Sn, ^{130}Te and ^{150}Nd isotopes for the $0^+(\text{gs}) \rightarrow 0^+(\text{gs})$ transition.

3.2 0ν ββ decay

In the light Majorana neutrino mass mechanism, the half-lives $T^{0\nu}_{1/2}$ for the $0^+ \rightarrow 0^+$ transition are given (in the closure approximation), by [19]

$$\left[T^{0\nu}_{1/2}\left(\beta^-\beta^-\right)\right]^{-1} = G_{01}\left(\beta^-\beta^-\right)\left|\frac{\langle m_\nu\rangle}{m_e}\right|^2 \times \left|\sum_{n,m}\left\langle 0^+_F\left\|\left[-\frac{H_F(r_{nm})}{g_A^2} + \sigma_n\cdot\sigma_m H_{GT}(r_{nm}) + S_{nm}H_T(r_{nm})\right]\tau^+_n\tau^+_m\right\|0^+_I\right\rangle\right|^2 \quad (2)$$

The neutrino potentials associated with Fermi, Gamow-Teller (GT) and tensor operators are given by

$$H_\alpha(r_{nm}) = \frac{2R}{\pi}\int \frac{f_\alpha\left(qr_{nm}\right)}{\left(q+\overline{A}\right)}\, h_\alpha(q) q dq$$

where $f_\alpha\left(qr_{nm}\right) = j_0\left(qr_{nm}\right)$ and $f_\alpha\left(qr_{nm}\right) = j_2\left(qr_{nm}\right)$ for α =Fermi/GT and tensor potentials, respectively.

The calculation of $M^{(0\nu)}$ in the PHFB model has been discussed in earlier works [12]. The effective Hamiltonian used is given by [12]

$$H = H_{sp} + V(P) + V(QQ) + V(HH) \quad (3)$$

where H_{sp}, $V(P)$, $V(QQ)$ and $V(HH)$ denote the single particle Hamiltonian, the pairing, quadrupole-quadrupole and hexadecapole-hexadecapole part of the effective two-body interaction, respectively.

Short range correlations and radial evolutions of NTMEs

In the literature, the short range correlations (SRC) have been included through the exchange of ω-meson [20], effective transition operator [21], unitary correlation operator method (UCOM) [22], self-consistent CCM [23] and phenomenological Jastrow type of correlations with Miller-Spenser parameterization [24]. Further, Šimkovic *et al.* [23] have shown that in the self-consistent CCM, it is possible to parametrize the effects of Argonne V18 and CD-Bonn nucleon-nucleon (NN) potentials by the Jastrow correlations with Miller-Spenser type of parameterization given by $f(r) = 1 - ce^{-ar^2}(1 - br^2)$. In the present work, the above form is adopted with $a = 1.1\ fm^{-2}$, $1.59\ fm^{-2}$, $1.52\ fm^{-2}$, $b = 0.68\ fm^{-2}$, $1.45\ fm^{-2}$, $1.88\ fm^{-2}$ and $c = 1.0$, 0.92, 0.46 for Miller-Spencer parameterization, Argonne V18 and CD-Bonn NN Potentials, which are denoted as SRC1, SRC2 and SRC3, respectively.

The inclusion of short range correlation (SRC) and finite size of nucleons with dipole form factor (F) induces an extra quenching in the NTMEs $M^{(0\nu)}$, which can range from the order of 18%–23% for SRC1 to negligible for SRC3. The dipole form factor (F) always reduces the NTMEs by 12%–15% in comparision to the point-particle case. Adding SRC (F + SRC) can further reduce the transition matrix elements for SRC1 or slightly enhance them, partially compensating for the effect of the dipole form factor. It is interesting to note that the effect of F+SRC2 is almost negligible, that is, nearly the same as F.

The radial evolution of $M^{(0\nu)}$ can be studied by defining

$$M^{(0\nu)} = \int C^{(0\nu)}(r)\, dr \qquad (4)$$

The radial evolution of $M^{(0\nu)}$ has been studied for four cases, namely F, F+SRC1, F+SRC2 and F+SRC3. To make the effects of finite size and SRC more transparent, we plot them for ^{100}Mo in Fig. 2. In case of finite sized nucleons, the $C^{(0\nu)}$ are peaked at $r \approx 1.25$ fm and with the inclusion of SRC1, SRC2 and SRC3, the position of peak remains unchanged. However, the magnitudes of $C^{(0\nu)}$ change in the latter three cases.

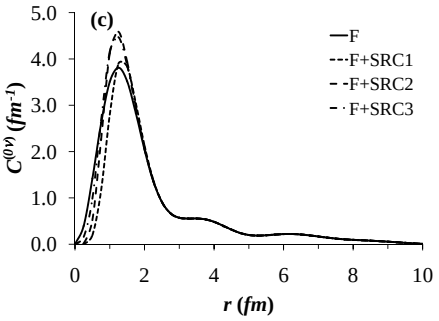

Figure 2 – Radial dependence of $C^{(0\nu)}(r)$ for the $\left(\beta^-\beta^-\right)_{0\nu}$ decay of ^{100}Mo isotope.

Table 1: Extracted limits on effective light Majorana neutrino mass $\langle m_\nu \rangle$ and predicted half lives using average NTMEs $\overline{M}^{(0\nu)}$ and uncertainties $\Delta\overline{M}^{(0\nu)}$ for the $\left(\beta^-\beta^-\right)_{0\nu}$ decay of ^{96}Zr, ^{100}Mo, ^{128,130}Te and ^{150}Nd isotopes.

$\beta^-\beta^-$ emitters	g_A	$\overline{M}^{(0\nu)}$	ISM [8]	(R)QRPA [23]	IBM [13]	G_{01} (10^{-14}y^{-1})	$T^{0\nu}_{1/2}(yr)$	Ref.	$\langle m_\nu \rangle$	$T^{0\nu}_{1/2}$(y) $< m_\nu >= 50\ meV$
^{100}Mo	1.254	7.22±0.50		2.91–5.56	3.732	4.640	4.6×10^{23}	[25]	$0.48^{+0.04}_{-0.03}$	$4.32^{+0.66}_{-0.54}\times10^{25}$
	1.0	7.94±0.58							$0.69^{+0.05}_{-0.05}$	$8.83^{+1.44}_{-1.15}\times10^{25}$
^{128}Te	1.254	4.22±0.31	2.26	3.21–5.65	4.517	0.1849	1.1×10^{23}	[26]	$8.50^{+0.67}_{-0.58}$	$3.18^{+0.52}_{-0.42}\times10^{27}$
	1.0	4.66±0.34							$12.10^{+0.94}_{-0.81}$	$6.44^{+1.04}_{-0.84}\times10^{27}$
^{130}Te	1.254	4.66±0.43	2.04	2.92–5.04	4.059	4.490	3.0×10^{24}	[27]	$0.30^{+0.03}_{-0.02}$	$1.07^{+0.23}_{-0.17}\times10^{26}$
	1.0	5.15±0.48							$0.42^{+0.04}_{-0.04}$	$2.17^{+0.47}_{-0.35}\times10^{26}$
^{150}Nd	1.254	3.24±0.44			2.321	21.16	1.8×10^{22}	[28]	$2.55^{+0.40}_{-0.31}$	$4.69^{+1.60}_{-1.06}\times10^{25}$
	1.0	3.59±0.50							$3.63^{+0.58}_{-0.44}$	$9.49^{+3.29}_{-2.16}\times10^{25}$

4 Uncertainty in NTMEs

4.1 Statistical uncertainties within PHFB model

In the study of both $(\beta\beta)_{2\nu}$ and $(\beta\beta)_{0\nu}$ decay modes, the renormalized value of axial vector coupling constant g_A is a major source of uncertainty. In the $(\beta\beta)_{0\nu}$ decay, the role of pseudoscalar

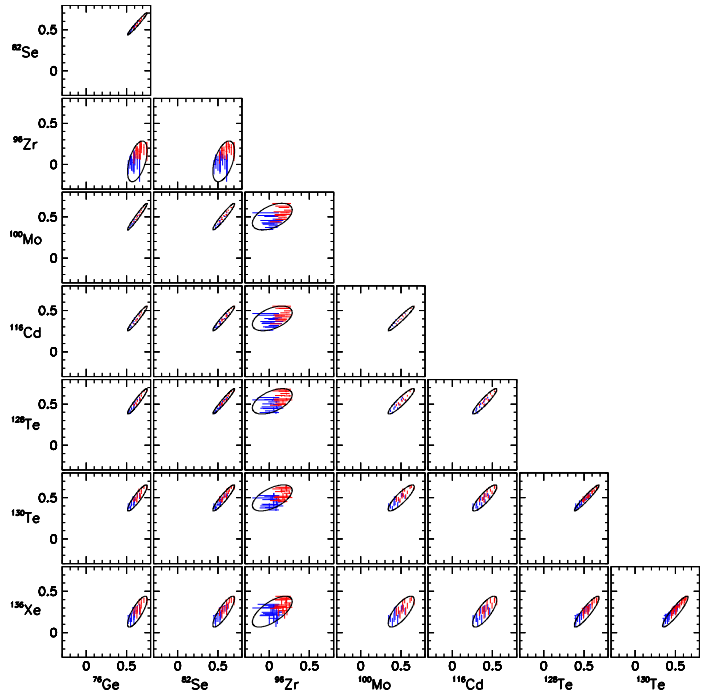

Figure 3 – Scatter plot of estimated QRPA values for logarithms of the $(\beta\beta)_{0\nu}$ matrix element for pairs of decaying nuclei, together with 1σ error ellipses. Reprinted from Ref. [29]; Copyright 2009 by the American Physical Society. Error bars on points indicate uncertainty in the QRPA parameter g_{pp}. Blue points are calculated with the Miller-Spencer treatment of short-range correlation functions and red points with the UCOM treatment.

and weak magnetism terms [19] is crucial, and the finite size of nucleons (FNS) and short range correlations (SRC) play a decisive role vis-a-vis the radial evolution of nuclear transition matrix elements (NTMEs) [8,12].

The uncertainties associated with the NTMEs $M^{(0\nu)}$ and $M^{(0N)}$ for $0\nu\beta\beta$ decay due to the exchange of light and heavy neutrinos, respectively are evaluated by calculating the mean and standard deviation as given by

$$\overline{M}^{(K)} = \frac{\sum_{i=1}^{N} M_i^{(K)}}{N} \quad \text{and} \quad \Delta\overline{M}^{(K)} = \frac{1}{\sqrt{N-1}} \left[\sum_{i=1}^{N} \left(\overline{M}^{(K)} - M_i^{(K)} \right)^2 \right]^{1/2}. \tag{5}$$

In Table 1, we have shown the average NTMEs and uncertainties for light Majorana neutrino mass mechanism. The predicted half-lives are given th Column 8 and compared with the available experimental results. The extracted values of light Majorana-ν mass are tabulated in column 10 of Table 1.

4.2 Statistical uncertainties within QRPA model

Due to large uncertainties in the systematics of nuclear matrix elements calculations, it is difficult to correctly analyze the statistical errors in nuclear matrix elements. However, efforts have been made to study uncertainties in $(\beta\beta)_{0\nu}$ matrix elements for various QRPA-like calculations by varying the value of g_A (1.0 and 1.25), the treatment of short range correlations (via the Miller-Spencer Jastrow function and the UCOM method), the size of the single-particle model space and the g_{pp} parameter (the most important parameter of QRPA model). The log of the nuclear matrix element in one nucleus versus the log of the matrix element in a second, for all possible pairs of nuclei are plotted in Fig. 3 (adopted from Ref. [29]). The error bar on each point representing the uncertainty in g_{pp}. The ellipses in the plot represent 1σ error in the matrix elements.

5 Conclusions

Reduction in uncertainty in NMEs first with in the different versions of a given model has to be reduced by trying to explain all possible systematics of experimental observation of nuclei involved in the DBD including intermediate nuclei. Any important physical processes that might have been ignored in earlier studies or the approximations used in past that might not be desirable for inclusion of short range correlations need to be explored and the effects studied. Finally different models have to include these effects and come to some possible consensus.

Acknowledgments

This work is partially supported by the Council of Scientific and Industrial Research (CSIR), India vide sanction No. 03(1216)/12/EMR-II, Indo-Italian Collaboration DST-MAE project via grant no. INT/Italy/P-7/2012 (ER) and Science and Engineering Research Board (SERB), DST vide sanction no. SB/S2/HEP-007/2013.

References

1. Y. Fukuda, et al., Phys. Rev. Lett. 81, 1562 (1998); Q. R. Ahmed, et al., Phys. Rev. Lett. 89, 011301 (2002); K. Eguchi, et al., Phys. Rev. Lett. 90, 021802 (2003).
2. W. H. Furry, Phys. Rev. 56, 1184 (1939).
3. H. Klapdor-Kleingrothaus et. al., Phys. Lett. B 586, 198 (2004).
4. M. Agostini et al. [GERDA Collaboration] Phys. Rev. Lett. 111, 122503 (2003); The EXO-200 Collaboration, Nature 510, 229 (2014).
5. O. Cremonesi, M. Pavan, Adv. High Eng. Phys. 2014, 951432 (2014).
6. S. M. Bilenky and C. Giunti, Int. J. Mod. Phys. A 30, 1530001 (2015).
7. J. Engel, J. Phys. G: Nucl. Part. Phys. 42, 034017 (2015).
8. E. Caurier, J. Menéndez, F. Nowacki, and A. Poves, Phys. Rev. Lett. **100**, 052503 (2008).
9. J. Suhonen and O. Civitarese, Phys. Rep. **300**, 123 (1998).
10. A. Faessler, and F. Šimkovic, J. Phys. G **24**, 2139 (1998).
11. D. Fang, A. Faessler, V. Rodin and F. Šimkovic, Phys. Rev. C **83**, 034320 (2011); Phys. Rev. C **82**, 051301(R) (2010) (references therein).
12. P. K. Rath et al., Phys. Rev. C. **85**, 014308 (2012); Phys. Rev. C. **88**, 064322 (2013) (references therein).
13. J. Barea and F. Iachello, Phys. Rev. C **79**, 044301 (2009).
14. T. R. Rodríguez and G. Martínez-Pinedo, Phys. Rev. Lett. **105**, 252503 (2010).
15. M. Doi, T. Kotani and E. Takasugi, Prog. Theor. Phys. Supp., **83** 1, (1985)
16. J. Kotila, F. Iachello, Phys. Rev. C 85, 034316 (2012); S. Stoica, M. Mirea, Phys. Rev. C 88, 037303 (2013).
17. A. S. Barabash, Phys. Rev. C 81, 035501 (2010).
18. A. S. Barabash, Nucl. Phys. A 935, 52 (2015).
19. J. D. Vergados, Phys. Rep. **361**, 1 (2002).
20. J. G. Hirsch, O. Castaños, and P. O. Hess, Nucl. Phys. A **582**, 124 (1995).
21. H. F. Wu et. al., Phys. Lett. **B162**, 227 (1985).
22. M. Kortelainen and J. Suhonen, Phys. Rev. C **76**, 024315 (2007); M. Kortelainen, O. Civitarese, J. Suhonen, and J. Toivanen, Phys. Lett. B **647**, 128 (2007).
23. F. Šimkovic et al., Phys. Rev. C **79**, 055501 (2009).
24. G. A. Miller and J. E. Spencer, Ann. Phys. (NY) **100**, 562 (1976).
25. R. Arnold *et al.*, Phys. Rev. Lett. **95**, 182302 (2005).
26. C. Arnaboldi *et al.*, Phys. Lett. **B557**, 167 (2003).
27. C. Arnaboldi *et al.*, Phys. Rev. C **78**, 035502 (2008).
28. J. Argyriades *et al.*, Phys. Rev. C **80**, 032501(R) (2009).
29. A. Faessler et. al., Phys. Rev. **D 79**, 053001 (2009).